

Synthesis, molecular structure and biological activity of novel bis-1,3-tropolones based on 4-chloro-2,7-dimethyl-1,8-naphthyridine

Evgeniy A. Gusakov,^{*a} Yurii A. Sayapin,^b Elena V. Vetrova,^a Ekaterina A. Lukbanova,^c Ekaterina V. Alilueva,^a Alexandra A. Kolodina,^a Valery V. Tkachev,^d Inna O. Tupaeva,^a Anton V. Lisovin,^a Dmitry V. Steglenko,^a Tatyana A. Krasnikova,^a Mikhail V. Nikogosov,^a Anna S. Goncharova,^e Anatoly V. Metelitsa,^a Sergey M. Aldoshin^d and Vladimir I. Minkin^a

^a Southern Federal University, 344090 Rostov-on-Don, Russian Federation. E-mail: egusakov@sedu.ru

^b Southern Scientific Center of the Russian Academy of Sciences, 344006 Rostov-on-Don, Russian Federation

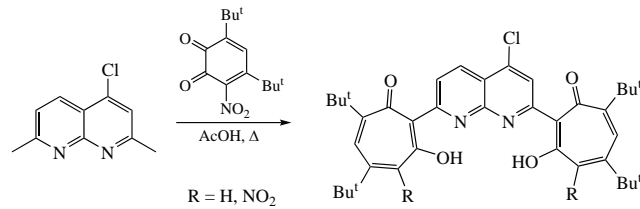
^c Don State Technical University, 344000 Rostov-on-Don, Russian Federation

^d Federal Research Center of Problems of Chemical Physics and Medicinal Chemistry, Russian Academy of Sciences, 142432 Chernogolovka, Moscow Region, Russian Federation

^e National Medical Research Center of Oncology, 344037 Rostov-on-Don, Russian Federation

DOI: 10.1016/j.mencom.2024.04.015

The acid-catalyzed reaction of 4-chloro-2,7-dimethyl-1,8-naphthyridine with 4,6-di-*tert*-butyl-3-nitro-1,2-benzoquinone leads to new bis-1,3-tropolones. The crystal structures of the obtained bis-1,3-tropolones were determined by X-ray diffraction analysis; the spectral and luminescent properties, the structural and energy characteristics of the compounds were examined. The cytotoxic effect *in vitro* against cancer cell lines A549, H1299, HT29, CT26 and B16F10 was assessed using MTT assay.



Keywords: 1,8-naphthyridine, 1,3-tropolone, X-ray diffraction analysis, fluorescence, solvatochromism, solid state emission, DFT, cytotoxic activity.

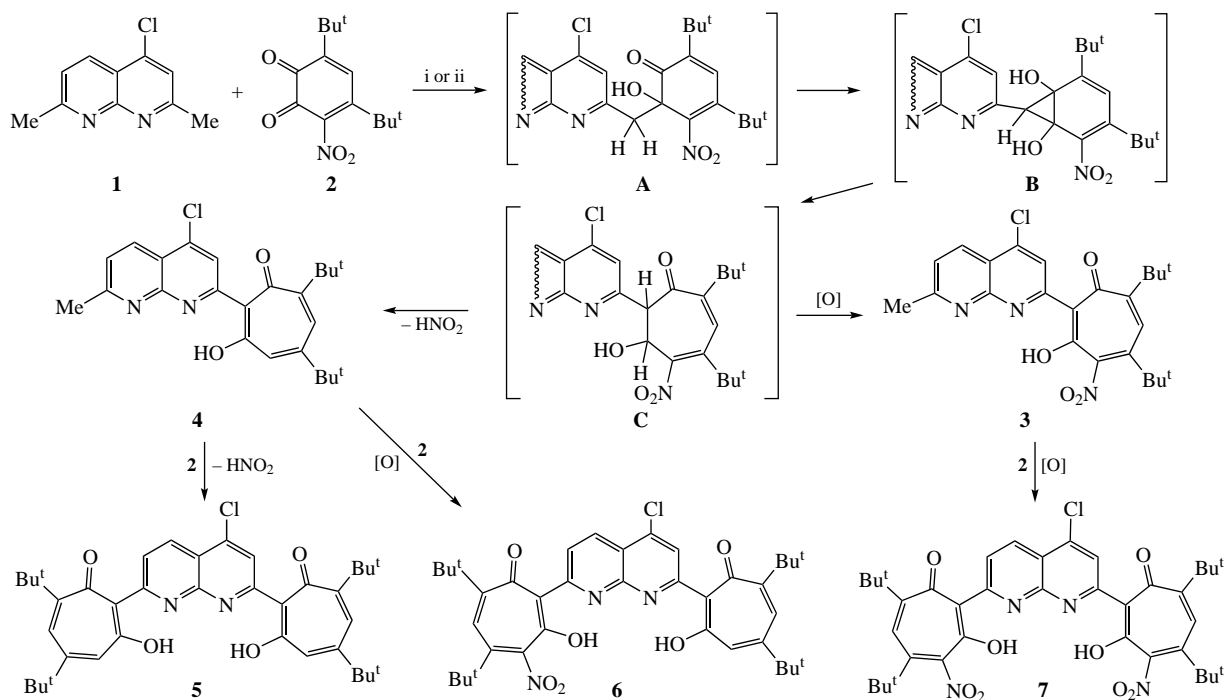
Compounds of the tropolone series that manifest a variety of pharmacological properties are of particular interest for medicinal chemistry. The high biological activity of troponoids is due to the presence of a pharmacophore center based on a seven-membered carbocyclic system. Tropolone derivatives exhibit high cytotoxic activity^{1–9} against lung cancer cell lines A549^{2,10–14} and H441,¹² ovarian cancer OVCAR-3 and OVCAR-8,¹² colon cancer HCT 116,¹⁴ pancreatic cancer Panc-1,¹² and breast cancer MCF7.^{1,2,15} 1,3-Tropolones based on benzoxazinone exhibit antibacterial properties against Gram-positive and Gram-negative antibiotic-resistant bacteria.¹⁶ Given the high biological activity of tropolones, the development of methods for the synthesis of derivatives belonging to this system is of current interest. One of the efficient approaches to 2-hetaryl-containing 1,3-tropolones is based on the expansion of the *o*-quinone ring in the reaction of 1,2-benzoquinones with 2-methyl-substituted nitrogen heterocycles to give 2-(quinolin-2-yl)-, 2-(quinoxalin-2-yl)- or 2-(benzazol-2-yl)-1,3-tropolones.^{17,18} Moreover, expansion of the *o*-quinone ring in the series of methylene-active naphthyridines by the reaction with quinones has not been studied so far. In our work, we report the first synthesis of substituted 2-naphthyridin-2-yl-1,3-tropolones by the reaction between 4-chloro-2,7-dimethyl-1,8-naphthyridine and 4,6-di-*tert*-butyl-3-nitro-1,2-benzoquinone.

We observed that the acid-catalyzed reaction of 4-chloro-2,7-dimethyl-1,8-naphthyridine **1** with 4,6-di-*tert*-butyl-3-nitro-1,2-benzoquinone **2** occurred with expansion of the *o*-quinone ring

to afford 3-hydroxy-5,7-di-*tert*-butyl-2-(7-methyl-4-chloro-1,8-naphthyridin-2-yl)-4-nitrotropone **3**, 2,2'-(4-chloro-1,8-naphthyridine-2,7-diyl)bis(5,7-di-*tert*-butyl-3-hydroxytropone) **5**, 5,7-di-*tert*-butyl-2-[5-chloro-7-(3-hydroxy-5,7-di-*tert*-butylcyclohepta-2,4,6-trienon-2-yl)-1,8-naphthyridin-2-yl]-3-hydroxy-4-nitrotropone **6** and 2,2'-(4-chloro-1,8-naphthyridine-2,7-diyl)bis(5,7-di-*tert*-butyl-3-hydroxy-4-nitrotropone) **7** (Scheme 1). The composition of the reaction mixture depends on the ratio of the starting reactants, since both methyl groups at positions 2 and 7 of 1,8-naphthyridine **1** are involved in the condensation to give bistropolones **5–7**. It is likely that the methyl group at position 2 of 1,8-naphthyridine is more reactive due to the presence of a chlorine atom at position 4 thus leading to the formation of monotropolones **3** and **4**.

The reaction with two equivalents of *o*-quinone **2** allowed 1,3-tropolone **3** and bis-1,3-tropolones **5–7** to be isolated. The presence of 1,3-tropolone **3** in the resulting reaction mixture is due to its incomplete conversion to **7** under conditions where *o*-quinone **2** is in deficiency. The formation of bis-1,3-tropolones **5** and **6** is possible in the reaction of 1,3-tropolone **4** with quinone **2** that produces trace amounts of **4** in the reaction mixture. The reaction with a fourfold excess of the original *o*-quinone **2** occurs more deeply: it involves the methyl group at position 7 and gives bistropolones **5–7** in 18–25% yields.

The mechanism of the formation of compounds **3–7** is presented in Scheme 1 and includes the step of aldol condensation of 4-chloro-2,7-dimethyl-1,8-naphthyridine **1**



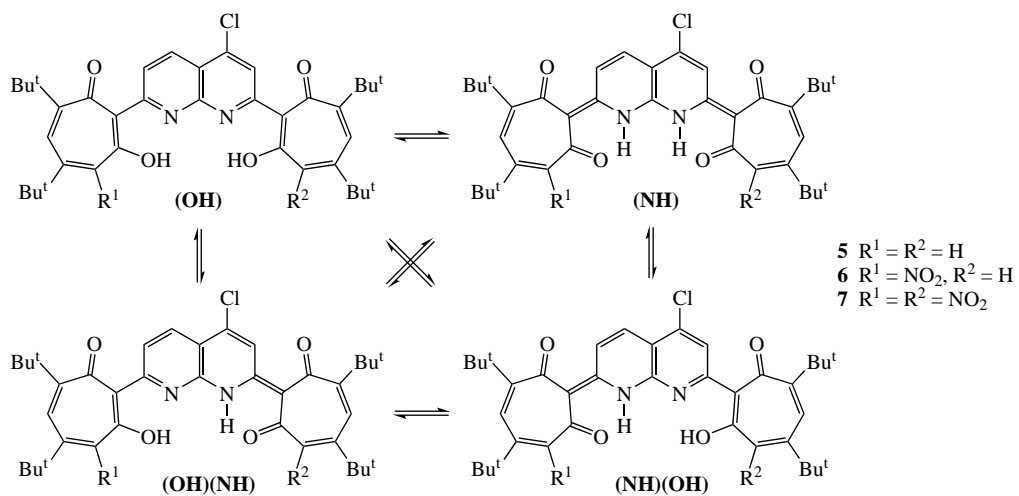
Scheme 1 Reagents and conditions: i, 2 (2 equiv.), AcOH, 80 °C, 25 h; ii, 2 (4 equiv.), AcOH, 80 °C, 45 h.

with 3-nitro-1,2-benzoquinone **2** to generate intermediate **A**, which undergoes cyclization to norcaradiene derivative **B**. Intermediate **B** rearranges into dihydrotropolone **C**, the oxidation of which with excess 3-nitro-1,2-benzoquinone **2** leads to 4-nitro-1,3-tropolone **3**. A competing reaction of the elimination of a nitrous acid molecule accompanied by a 1,3-sigmatropic shift of a hydrogen atom results in 1,3-tropolone **4**. The formation of bistropolone **7** is possible in the further reaction of tropolone **3** with **2** *via* the same mechanism with expansion of the *o*-quinone ring (see Scheme 1) involving the oxidation of the intermediate dihydrotropolone with excess compound **2**. The further reaction of tropolone **4** with quinone **2** occurs both by elimination of a nitrous acid molecule to give bistropolone **5** and by oxidation with excess of the initial quinone **2** to yield bistropolone **6**.

The structures of the resulting compounds **3**, **5**–**7** were determined by ^1H , ^{13}C , ^{15}N , COSY, HMQC and HMBC two-

dimensional heteronuclear NMR spectroscopy, IR spectroscopy, mass spectrometry and elemental analysis (see Online Supplementary Materials, Figures S1–S16, Table S1). Analysis of 2D correlation NMR spectra has shown that compound **6** exists in the (NH)(OH) tautomeric form in chloroform solution (Figure S3, Scheme 2). In fact, the ^1H – ^{15}N HMBC spectrum of compound **6** contains cross-peaks of the N(8') nitrogen atom at δ 173.4 with protons δ_{H} 17.95 and H(6") δ_{H} 8.14, while the ^1H – ^{13}C HMBC spectrum contains cross-peaks of the NH proton δ_{H} 17.95 with C(6"), C(4'a), C(2") atoms at δ_{H} 120.2, 116.4, 114.9, respectively. Thus, a proton shift to the pyridine nitrogen of naphthyridine is observed in the nitro-substituted tropolone ring of molecule **6**.

The structures of bistropolone derivatives **5** and **7** were confirmed by X-ray diffraction analysis (Figures 1 and 2).[†] The main experimental and crystallographic data, as well as the



Scheme 2 Tautomeric forms of compounds 5–7.

[†] Crystal data for **5**. $\text{C}_{38}\text{H}_{45}\text{N}_2\text{O}_4\text{Cl}$ (M_f = 629.21), monoclinic, space group $P1$, a = 9.6816(9), b = 12.1524(12) and c = 15.9775(16) Å, α = 107.492(9), β = 104.677(8) and γ = 94.924(8)°, V = 17074.4(3) Å³, Z = 2, d_{calc} = 1.224 g cm⁻³, $\mu(\text{MoK}_\alpha)$ = 0.154 mm⁻¹, 14757 reflections measured,

9132 unique (R_{int} = 0.0714, R_{sigma} = 0.1284) which were used in all calculations. The final R_1 was 0.1696 [$I > 2\sigma(I)$] and wR_2 was 0.4849 (all data).

Crystal data for **7**. $\text{C}_{38}\text{H}_{43}\text{N}_4\text{O}_8\text{Cl}$ (M_f = 719.21), rhombic, space group $Pbca$, a = 19.5970(7), b = 12.8733(6) and c = 29.2894(12) Å,

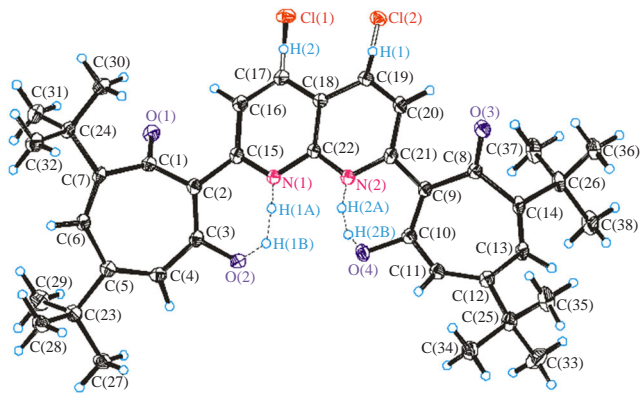


Figure 1 Molecular structure of 2,2'-(4-chloro-1,8-naphthyridine-2,7-diy)bis(5,7-di-tert-butyl-3-hydroxytropone) **5**.

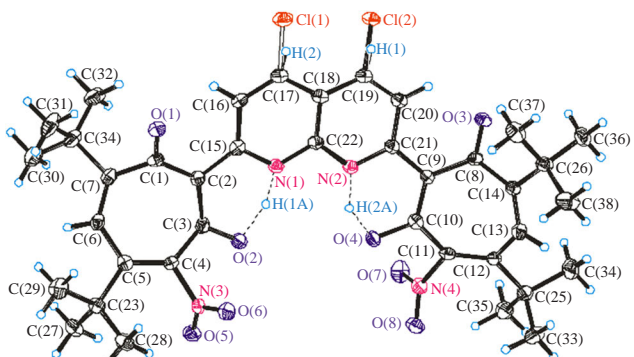


Figure 2 Molecular structure of 2,2'-(4-chloro-1,8-naphthyridine-2,7-diy)bis(5,7-di-tert-butyl-3-hydroxy-4-nitropropone) **7**.

distances and angles in the molecule, are given in Tables S2–S9 (Online Supplementary Materials). First of all, it is necessary to note the statistical distribution of chlorine atoms and the corresponding arrangement of hydrogen atoms at the C(17) and C(19) atoms in both bistropoles **5** and **7** in the 0.5:0.5 and 0.6:0.4 ratios, respectively. The second thing that draws attention is the distribution of hydrogen atoms in positions between the N(1) and O(2) atoms; [N(2) and O(4)] with some difference, *i.e.*, in compound **5** the positions of hydrogen atoms are separated by two tautomers at the nitrogen atom and at the oxygen atom (Figure 1), as noted elsewhere,¹⁹ while in bistropolone **7** it is localized in an intermediate position. The tropolone rings retain a ‘bath’ configuration with bends along the C(2)…C(7), C(9)…C(14) and C(3)…C(6), C(10)…C(13) lines.

The UV-VIS and luminescent properties of symmetric bistropolones **5** and **7** were studied in solution (heptane, toluene, chloroform, THF and MeCN, and EtOH) and in solid state (Table S10, Figures S19–S26). The long-wave absorption band of **5** is characterized by a peak at 452–456 nm with a molar extinction coefficient of 26 700–30 800 $\text{dm}^3 \text{ mol}^{-1} \text{ cm}^{-1}$. The photoluminescence spectrum of **5** is structured and shows maxima at 519–523 and 541–556 nm (see Figures S19–S22). In all the solutions studied, the fluorescence excitation spectrum of **5** corresponds to the shoulder at position 494–509 nm in the corresponding absorption spectra. The results indicate the

$V = 7389.1(5) \text{ \AA}^3$, $Z = 8$, $d_{\text{calc}} = 1.293 \text{ g cm}^{-3}$, $\mu(\text{MoK}_\alpha) = 0.160 \text{ mm}^{-1}$, 19714 reflections measured, 7300 unique ($R_{\text{int}} = 0.0826$, $R_{\text{sigma}} = 0.1167$) which were used in all calculations. The final R_1 was 0.0739 [$I > 2\sigma(I)$] and wR_2 was 0.2102 (all data).

CCDC 2041292 (**5**) and 2041318 (**7**) contain the supplementary crystallographic data for this paper. These data can be obtained free of charge from The Cambridge Crystallographic Data Centre *via* <http://www.ccdc.cam.ac.uk>.

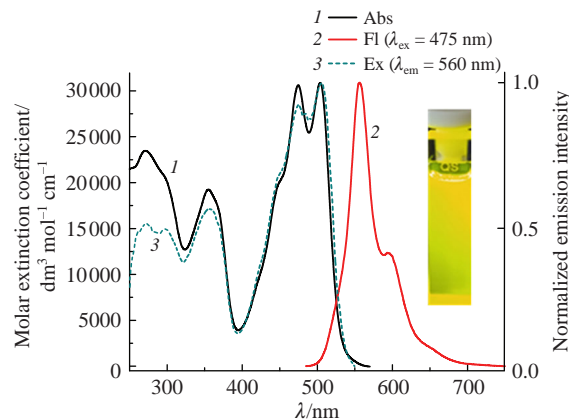


Figure 3 Absorption, emission and excitation spectra of compound **7** in chloroform. A photo of the solution under UV irradiation (365 nm).

presence of two tautomeric forms of compound **5** in solution, one of which exhibits fluorescence (see Table S10). The increase in the intensity of the shoulder at 494–509 nm with an increase in solvent polarity (from 6800 in heptane to 12 500 $\text{dm}^3 \text{ mol}^{-1} \text{ cm}^{-1}$ in MeCN) denotes that the equilibrium of the dominant OH-form of bistropolone in solution shifts toward the formation of a fluorescent tautomeric NH form. At the same time, the value of the Stokes shift is the smallest in heptane (378 cm^{-1}), which indicates that the molecular structure of fluorescent tautomer **5** stabilizes in the nonpolar solvent. An increase in the solvent polarity leads to a significant increase in the excitation energy loss to reach 1205 cm^{-1} in EtOH.

The absorption spectrum of bistropolone **7** in aprotic solvents is characterized by a long-wave transition band with a pronounced vibrational structure with peaks at 470–475 and 497–505 nm (see Table S10, Figures S23–S25). The fluorescence of **7** is localized at 547–557 nm (Figures 3 and S23–S25). The fluorescence quantum yields of **7** decrease on passage from nonpolar to polar solvents (from 0.06 in toluene to 0.004 in EtOH). In contrast to **5**, incorporation of an acceptor group (NO_2) results in an increase in the solvatochromic sensitivity of compound **7**. Both compounds **5** and **7** exhibit single-band fluorescence in the solid state with close emission maxima localized at 578 and 573 nm, respectively (Figure 4). The quantum yield of the solid-state fluorescence of **7** is higher than that in solutions (see Table S10).

The possible tautomeric forms of compounds **5–7** are shown in Scheme 2, and those for compound **3** are shown in Figure S27. The thermodynamic equilibrium between them in the gas phase and in a polar solvent (DMSO) was studied by a theoretical DFT method (B3LYP) with the standard 6-311++G(d,p) basis

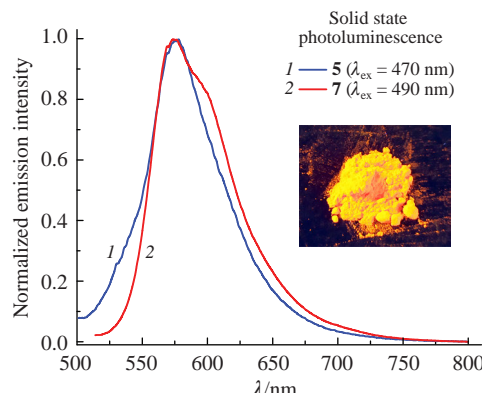


Figure 4 Emission spectra of compounds **5** and **7** in solid state (as powders). A photo of compound **7** under UV irradiation (365 nm).

(Tables 1, S11–S18 and Figures S27–S30). As shown previously,¹² the equilibrium of the (NH) and (OH) tautomeric forms of tropolone derivatives is mainly affected, on the one hand, by the donor–acceptor properties of the molecule fragments, and on the other hand, by the polarity of the medium. Varying these factors makes it possible to change the equilibrium of the isomers in a wide range. According to the earlier results, the (OH)-form often predominated in compounds incorporating quinoline and tropolone moieties.¹²

In this study, quantum-chemical calculations have shown that replacement of the quinoline moiety by a naphthyridine one results in significant stabilization of the (NH)-form of compound **3** (Table 1). This effect is enhanced even further in the polar solvent (DMSO). Incorporation of a second tropolone moiety causes stabilization of the OH-form, while the (OH)(NH) and (NH)(OH) forms are nearly equal in energy. A polar solvent destabilizes the (OH)-form of compound **5**. The presence of a nitro group in the left-hand tropolone moiety stabilizes the (NH)(OH) isomer significantly. In the gas phase, the NH-form is not localized, but in the polar solvent, the (OH), (OH)(NH) and (NH)(OH) tautomers of **6** are almost equal in energy. Incorporation of a nitro group into the right-hand tropolone moiety stabilizes the (OH)(NH) isomer. As a result, the energies of the (OH)(NH) and (NH)(OH) isomers become nearly equal (see Table 1, compound **7**). In a polar solvent (DMSO), this effect is enhanced further.

It has been shown¹² that tropolones in the tautomeric aminoenone (NH) form manifested a high cytotoxic effect against various cancer cell lines, and it is probably the tautomeric (NH)-form that was involved in the mechanisms of cancer cell growth inhibition. According to quantum-chemical calculations (see Table 1), compounds **3**, **6**, **7** exist in the tautomeric (NH) form in the polar solvent, which makes it possible to assume that these compounds should possess anticancer properties. The most synthetically available bistropolone **7** containing nitro groups was used for further biological tests. Bistropolone **7** was examined for *in vitro* cytotoxic activity against the following cell lines: human non-small cell lung cancer A549 and H1299, human colon cancer HT29, mouse colon cancer CT26 and mouse melanoma B16F10. The half-inhibition concentration IC_{50} was determined in the cytotoxicity assessments. The results on the cytotoxic activity of bistropolone **7** at various concentrations are summarized in Table S19 (see Online Supplementary Materials).

Table 1 Total energies with zero-point energy correction $E_{\text{tot}} + \text{ZPE}$ (arbitrary units) and relative energies ΔE of isomers of tropolone derivatives **3**, **5**–**7** in the gas phase (g) and in DMSO solution (s) according to B3LYP/6-311++G(d,p) calculations.

Compound	Tautomer	Energy characteristics/kcal mol ⁻¹			
		$E_{\text{tot}} + \text{ZPE}$ (g)	ΔE (g)	$E_{\text{tot}} + \text{ZPE}$ (s)	ΔE (s)
3	(OH)	−1855.38879	0.0	−1855.40578	0.0
	(NH)	−1855.39280	−2.5	−1855.41150	−3.6
5	(OH)	−2345.51351	0.0	−2345.5297	0.0
	(NH)	−2345.50686	4.2	−2345.52552	2.6
6	(OH)(NH)	−2345.51142	1.31	−2345.52923	0.30
	(NH)(OH)	−2345.51149	1.27	−2345.52933	0.23
7	(OH)	−2550.04967	0.0	−2550.07044	0.0
	(NH)	−	−	−2550.06987	0.4
	(OH)(NH)	−2550.04689	1.7	−2550.06911	0.8
	(NH)(OH)	−2550.05171	−1.3	−2550.07429	−2.4
	(OH)	−2754.58498	0.0	−2754.61064	0.0
	(NH)	−2754.58355	0.90	−2754.61343	−1.75
	(OH)(NH)	−2754.58625	−0.797	−2754.61389	−2.039
	(NH)(OH)	−2754.58627	−0.810	−2754.61387	−2.027

The IC_{50} values for different cancer cell lines are presented in Figure S31, where the indicated results are the mean values from three independent experiments. Compound **7** was found to exhibit inhibitory activity with a pronounced dose-dependent cytotoxic effect against all the five cell lines. The strongest antiproliferative activity, $IC_{50} = 22.5 \mu\text{g ml}^{-1}$, was shown against the HT29 human colon cancer culture. The IC_{50} values for the other cancer cell lines were slightly higher and amounted to $27.16 \mu\text{g ml}^{-1}$ (A549), $27.14 \mu\text{g ml}^{-1}$ (H1299), $31.17 \mu\text{g ml}^{-1}$ (CT26) and $31.73 \mu\text{g ml}^{-1}$ (B16F10).

In conclusion, the reaction of 4,6-di-*tert*-butyl-3-nitro-1,2-benzoquinone **2** with 4-chloro-2,7-dimethyl-1,8-naphthyridine **1** affords new 1,3-tropolone **3** and bis-1,3-tropolones **5**–**7**. Analysis of the UV-VIS and luminescence characteristics showed that these compounds exhibited fluorescence both in solutions and in the solid state. Bistropolone **5** undergoes a tautomeric transformation that depends on the polarity of the solvent. In contrast to compound **5**, incorporation of an acceptor group (NO_2) results in an increase in the solvatochromic sensitivity of bistropolone **7**. Quantum-chemical calculations show that the presence of a nitro group in the tropolone ring stabilizes the NH tautomeric forms, which is consistent with the data of two-dimensional heteronuclear NMR and X-ray diffraction analyses of bistropolones **5** and **7**. *In vitro* cytotoxic activity against five different cancer cell lines was revealed for bistropolone **7**; the bistropolone demonstrated the most pronounced antitumor effect against HT29 human colon cancer culture.

This study was supported by the Russian Science Foundation (grant no. 21-73-10300, <https://rscf.ru/project/21-73-10300/>), and was carried out at Southern Federal University. X-ray diffraction studies were performed in accordance with the state task (State registration no. AAAA-A19-119092390076-7, Valery V. Tkachev, Sergey M. Aldoshin).

Online Supplementary Materials

Supplementary data associated with this article can be found in the online version at doi: 10.1016/j.mencom.2024.04.015.

References

- J. Kornakulkarn, S. Saepua, R. Suvannakad, S. Supothina, N. Boonyuen, M. Isaka, S. Prabpai, P. Kongsaeree and C. Thongpanchang, *Tetrahedron*, 2017, **73**, 3505.
- J. Krzywik, M. Aminpour, J. Janczak, E. Maj, M. Moshari, W. Mozga, J. Wietrzyk, J. A. Tuszyński and A. Huczycski, *Eur. J. Med. Chem.*, 2021, **215**, 113282.
- J. Zhang, L. Liu, B. Wang, Y. Zhang, L. Wang, X. Liu and Y. Che, *J. Nat. Prod.*, 2015, **78**, 3058.
- K.-C. Wei, R.-F. Chen, Y.-F. Chen and C.-H. Lin, *Toxicol. Appl. Pharmacol.*, 2019, **366**, 35.
- S. L. Haney, M. L. Varney, H. R. Safranek, Y. S. Chhonker, N. G. Dayanandan, G. Talmon, D. J. Murry, A. J. Wiemer, D. L. Wright and S. A. Holstein, *Leuk. Res.*, 2019, **77**, 17.
- C.-C. Wang, B.-K. Chen, P.-H. Chen and L.-C. Chen, *Taiwan. J. Obstet. Gynecol.*, 2020, **59**, 698.
- J. Kurek, P. Kwasniewska-Sip, K. Myszkowski, G. Cofta, P. Barczyński, M. Murias, R. Kurczab, P. Śliwa and P. Przybylski, *Chem. Biol. Drug Des.*, 2019, **94**, 1930.
- S. L. Haney, C. Allen, M. L. Varney, K. M. Dykstra, E. R. Falcone, S. H. Colligan, Q. Hu, A. M. Aldridge, D. L. Wright, A. J. Wiemer and S. A. Holstein, *Oncotarget*, 2017, **8**, 76085.
- G. Zhang, J. He, X. Ye, J. Zhu, X. Hu, M. Shen, Y. Ma, Z. Mao, H. Song and F. Chen, *Cell Death Dis.*, 2019, **10**, 255.
- C.-J. Hsiao, S.-H. Hsiao, W.-L. Chen, J.-H. Guh, G. Hsiao, Y.-J. Chan, T.-H. Lee and C.-L. Chung, *Chem.-Biol. Interact.*, 2012, **197**, 23.
- O. I. Kit, V. I. Minkin, E. A. Lukbanova, Yu. A. Sayapin, E. A. Gusakov, A. O. Sitkovskaya, S. Y. Filippova, E. F. Komarova, A. V. Volkova, D. V. Khodakova, M. V. Mindar, Yu. N. Lazutin, M. A. Engibaryan and V. E. Kolesnikov, *Bull. Sib. Med.*, 2022, **21** (2), 60.

12 E. A. Gusakov, I. A. Topchu, A. M. Mazitova, I. V. Dorogan, E. R. Bulatov, I. G. Serebriiskii, Z. I. Abramova, I. O. Tupaeva, O. P. Demidov, N. T. Duong, D. L. Tran, N. B. Duong, Y. A. Boumber, Y. A. Sayapin and V. I. Minkin, *RSC Adv.*, 2021, **11**, 4555.

13 Z. Y. Al Subeh, N.-Q. Chu, J. T. Korunes-Miller, L. L. Tsai, T. N. Graf, Y. P. Hung, C. J. Pearce, M. W. Grinstaff, A. H. Colby, Y. L. Colson and N. H. Oberlies, *J. Controlled Release*, 2021, **331**, 260.

14 Q.-G. Ma, R.-R. Wei, X.-D. Zhang, Z.-P. Sang, J.-H. Dong, Q.-X. Lu, H.-F. Huang, D.-M. Guo and L. Jiang, *Fitoterapia*, 2020, **146**, 104.

15 L. M. Balsa, M. C. Ruiz, L. S. M. de la Parra, E. J. Baran and I. E. Leyn, *J. Inorg. Biochem.*, 2020, **204**, 1109.

16 Yu. A. Sayapin, E. A. Gusakov, I. V. Dorogan, I. O. Tupaeva, M. G. Teimurazov, N. K. Fursova, K. V. Ovchinnikov and V. I. Minkin, *Russ. J. Bioorg. Chem.*, 2016, **42**, 224 (*Bioorg. Khim.*, 2016, **42**, 247).

17 V. I. Minkin, S. M. Aldoshin, V. N. Komissarov, I. V. Dorogan, Yu. A. Sayapin, V. V. Tkachev and A. G. Starikov, *Russ. Chem. Bull.*, 2006, **55**, 2032 (*Izv. Akad. Nauk, Ser. Khim.*, 2006, 1956).

18 Y. A. Sayapin, I. O. Tupaeva, A. A. Kolodina, E. A. Gusakov, V. N. Komissarov, I. V. Dorogan, N. I. Makarova, A. V. Metelitsa, V. V. Tkachev, S. M. Aldoshin and V. I. Minkin, *Beilstein J. Org. Chem.*, 2015, **11**, 2179.

19 V. V. Tkachev, Yu. A. Sayapin, G. V. Shilov, V. N. Komissarov, S. M. Aldoshin and V. I. Minkin, *J. Struct. Chem.*, 2016, **57**, 622 (*Zh. Strukt. Khim.*, 2016, **57**, 652).

Received: 13th December 2023; Com. 23/7344